# Activated monocytes in peritumoral stroma of hepatocellular carcinoma foster immune privilege and disease progression through PD-L1

Dong-Ming Kuang,[1] Qiyi Zhao,[1] Chen Peng,[1] Jing Xu,[1] Jing-Ping Zhang,[1] Changyou Wu,[2] and Limin Zheng[1,3]

[1]State Key Laboratory of Biocontrol, [2]Department of Immunology, and [3]State Key Laboratory of Oncology in Southern China, Sun Yat-Sen University, Guangzhou 510 275, China

**Macrophages (Mφ) are prominent components of solid tumors and exhibit distinct phenotypes in different microenvironments. We have recently found that tumors can alter the normal developmental process of Mφ to trigger transient activation of monocytes in peritumoral stroma. We showed that a fraction of monocytes/Mφ in peritumoral stroma, but not in cancer nests, expresses surface PD-L1 (also termed B7-H1) molecules in tumors from patients with hepatocellular carcinoma (HCC). Monocytes activated by tumors strongly express PD-L1 proteins with kinetics similar to their activation status, and significant correlations were found between the levels of PD-L1$^+$ and HLA-DR$^{high}$ on tumor-infiltrating monocytes. Autocrine tumor necrosis factor α and interleukin 10 released from activated monocytes stimulated monocyte expression of PD-L1. The PD-L1$^+$ monocytes effectively suppressed tumor-specific T cell immunity and contributed to the growth of human tumors in vivo; the effect could be reversed by blocking PD-L1 on those monocytes. Moreover, we found that PD-L1 expression on tumor-infiltrating monocytes increased with disease progression, and the intensity of the protein was associated with high mortality and reduced survival in the HCC patients. Thus, expression of PD-L1 on activated monocytes/Mφ may represent a novel mechanism that links the proinflammatory response to immune tolerance in the tumor milieu.**

CORRESPONDENCE
Limin Zheng:
zhenglm@mail.sysu.edu.cn

Abbreviations used: DFS, disease-free survival; HCC, hepatocellular carcinoma; MFI, mean fluorescence intensity; Mφ, macrophages; NOD/SCID, nonobese diabetic/severe combined immunodeficiency; OS, overall survival; rh, recombinant human; TSN, tumor culture supernatant.

Tumor progression is now recognized as the product of evolving cross talk between different cell types within the tumor and its stroma (1, 2). Although normal stroma is nonpermissive for neoplastic progression, cancer cells can modulate adjacent stroma to generate a supportive microenvironment (1–3). This includes the ability to alter the ratios of effector to regulatory T cells and to affect the functions of APCs and the expression of cosignaling molecules, which in turn creates an immunosuppressive network to promote tumor progression and immune evasion (3, 4). There is also emerging evidence that the proinflammatory response at the tumor stroma can be rerouted in a tumor-promoting direction (5). These observations suggest that different tumor microenvironments can create either immune suppression or activation at distinct sites to promote tumor progression.

Macrophages (Mφ) constitute a major component of the leukocyte infiltrate in tumor stroma. These cells are derived almost entirely from circulating monocytes, and in response to environmental signals, they acquire special phenotypic characteristics that are associated with diverse functions (6–8). We have recently found that tumor environments can alter the normal development of Mφ that is intended to trigger transient early activation of monocytes in the peritumoral region (7). Furthermore, in a study of patients with hepatocellular carcinoma (HCC) (5), it was noted that an increased number of activated monocytes/Mφ (HLA-DR$^{high}$CD68$^+$ cells) in the liver was associated with progression



The Rockefeller University Press $30.00
J. Exp. Med. Vol. 206 No. 6 1327-1337
www.jem.org/cgi/doi/10.1084/jem.20082173



The Journal of Experimental Medicine

of the disease. Thus, immune functional data of activated monocytes/Mφ in cancer environments are essential for understanding their roles and potential mechanisms in tumor immunopathogenesis.

PD-L1 (also termed B7-H1 and CD274) is a member of the B7 family of cosignaling molecules, and it possesses the dual functions of co-stimulation of naive T cells via an as yet unidentified receptor and coinhibition of activated effector T cells through PD-1 receptor (4, 9, 10). Expression of PD-L1 (B7-H1) is often induced or maintained by many inflammatory cytokines (4, 11), of which IFN-γ is the most potent. In addition to being expressed on activated immune cells, most human cancers also express high levels of PD-L1 (B7-H1) protein, which correlates with poor prognosis in some cases (4, 11–13). In contrast, low or rare PD-L1 (B7-H1) expression is observed in most mouse and human tumor cell lines, possibly because of the lack of a complete cancer microenvironment in cell lines in vitro (4, 12). At present, little is known about the expression and function of PD-L1 (B7-H1) on APCs in the inflammatory activated stroma of human tumors in situ.

HCC is the fifth most common cancer worldwide, with an extremely poor prognosis (14). By using HCC as a model system, the present study showed that PD-L1$^+$ monocytes were accumulated in the peritumoral stroma area of cancers and increased with tumor progression. The pattern of PD-L1 (B7-H1) expression coincided with the transient activation of monocytes/Mφ during their initial exposure to the tumor environment. These activated PD-L1$^+$ monocytes suppressed tumor-specific T cell immunity, and their high infiltration was associated with poor survival of the HCC patients. Moreover, we found that blocking PD-L1 (B7-H1) effectively attenuated this monocyte-mediated T cell anergy and restored their antitumor activity in vivo. Therefore, PD-L1 (B7-H1) expression on activated monocytes may represent a novel mechanism by which the proinflammatory response is linked to immune tolerance in the tumor milieu.

## RESULTS

### PD-L1$^+$ monocytes are highly enriched in the peritumoral stroma of HCC patients

To evaluate the potential role of PD-L1 in tumor immunopathology, we examined surface expression of this protein on circulating leukocytes from HCC patients and healthy donors, and on infiltrating leukocytes freshly isolated from tumor and nontumor liver tissues of patients with various stages of HCC ($n$ = 28 in each group). In all of the samples analyzed, 92 ± 7% of the PD-L1$^+$ leukocytes were CD14$^{high}$ cells that were considered as monocytes. PD-L1 was weakly expressed on a fraction of circulating monocytes in both healthy donors and patients. Although the percentage of PD-L1$^+$ cells was increased in nontumor-infiltrating monocytes, their intensity of PD-L1 expression was low. Compared with nontumor-infiltrating monocytes, the monocytes isolated from the corresponding tumor tissues comprised a significantly greater proportion of PD-L1$^+$CD14$^{high}$ cells and expressed significantly larger amounts of PD-L1 (both $P < 0.0001$; Fig. 1, A–C). Moreover, we found that the ratios of PD-L1$^+$CD14$^{high}$ cells in both nontumor and tumor-derived monocytes were higher in advanced stage HCC patients (stages III and IV; $n$ = 13) than those in early stages (stages I and II; $n$ = 15; $P < 0.05$ for nontumor and $P < 0.001$ for tumor tissues; Fig. 1, A and B).

We subsequently examined the distribution of PD-L1$^+$ cells in HCC samples. Using confocal microscopy, we confirmed that PD-L1 protein was expressed mainly on CD68$^+$ monocytes/Mφ ($n$ = 10) and was only weakly expressed on other stromal and hepatoma cells (Fig. 1 D). Interestingly, only CD68$^+$ cells in the peritumoral stroma showed marked expression of PD-L1, whereas most CD68$^+$ cells in the cancer nests were weakly expressed or negative for PD-L1 (Fig. 1 D). Collectively, these data indicate that PD-L1 is selectively expressed on monocytes/Mφ in peritumoral stroma at levels that increase with progressive stages in HCC patients.

### Tumor environmental factors induce early transient expression of PD-L1 on monocytes

We have recently shown that tumor microenvironments may co-opt the normal development of Mφ to dynamically educate the recruiting monocytes in different niches of a tumor (7). To investigate whether such mechanisms are also responsible for selective expression of PD-L1 on monocytes/Mφ in peritumoral stroma, we incubated normal blood monocytes with supernatants from cultures of hepatoma or normal liver cell lines. Exposure to 15% tumor culture supernatants (TSNs) from hepatoma (SK-Hep-1 and HepG2) cells induced rapid expression of PD-L1 on monocytes, reaching a maximum within 36 h and then gradually declining (Fig. 2 A). On day 7, TSN-exposed Mφ displayed significantly reduced expression of PD-L1. In contrast, supernatant from normal liver cells (LO2) had only a marginal effect on PD-L1 expression by monocytes/Mφ, even when used at a high concentration (30%).

APCs are more susceptible to express PD-L1 when they are activated (4, 15); hence, we examined the activation status of TSN-exposed monocytes at their early or later differentiation stage. The results showed that the expression of HLA-DR, CD80, and CD86 was significantly up-regulated on monocytes after exposure to TSNs from hepatoma cells for 24 h, but was reduced on day 7 when the cells developed into Mφ (Fig. 2 B). Similar patterns of cytokine productions were obtained in TSN-exposed monocytes, including the accumulations of TNF-α, IL-10, IL-6, IL-12, and IL-1β in the culture media at their early differentiation stage and a subsequent decline on day 7 (Fig. 2 C). Furthermore, comparison of the kinetics of PD-L1 expression and cytokine production in TSN-exposed monocytes revealed that cytokine profiles preceded PD-L1 expression (Fig. 2 A) (7). These findings suggest that TSN-induced activation of monocytes led to expression of PD-L1. The TSNs we used did not contain any measurable levels of TNF-α, IL-10, IL-1β, or IL-12, except for a low concentration of IL-6 (227 ± 53 pg/ml).

### Autocrine cytokines from activated monocytes induce expression of PD-L1

Cytokines derived from myeloid cells have previously been found to induce expression of PD-L1 in human tumor DCs (11). To ascertain whether autocrine cytokines from activated monocytes contribute to the expression of PD-L1, we used specific neutralizing antibodies to abolish the effects of TNF-α, IL-10, or IL-6. As expected, blocking IL-10 effectively inhibited the up-regulation of PD-L1 protein (Fig. 2 D). Interestingly, monocyte PD-L1 expression was also partially attenuated by the anti–TNF-α antibody, whereas it was not affected by treatment with a concentration of anti–IL-6 antibody that effectively neutralized IL-6 in the culture system (Fig. 2 D and Table S1). To gain further support for roles of TNF-α and IL-10 in induction of PD-L1 on monocytes, we tested recombinant human (rh) cytokines in the culture system. As shown in Fig. 2 E, rhIL-10 induced significant expression of PD-L1 on monocytes in a dose-dependent manner. Although rhTNF-α alone, at concentrations up to 10 ng/ml, only had a marginal effect, it did synergistically increase the IL-10–mediated PD-L1 expression on monocytes (Fig. 2 E). These findings imply that IL-10 is involved in PD-L1 expression on human monocytes, and that effect can be potentiated by TNF-α.

We have recently observed that hyaluronan fragments constitute a common factor produced by several types of human tumors, including hepatoma, to stimulate the production of TNF-α and IL-10 (7, 16). Therefore, we examined whether hyaluronan fragments are involved in inducing expression of PD-L1 on monocytes. The results showed that the up-regulation of PD-L1 protein on TSN-exposed monocytes was significantly impaired both by adding a hyaluronan-specific blocking peptide (Pep-1) (16–18) and by reducing hyaluronan levels in TSNs via silencing of hyaluronan synthase 2 in tumor cells (Fig. 2 D), both of which have been shown to attenuate the release of TNF-α and IL-10 by these monocytes (7).

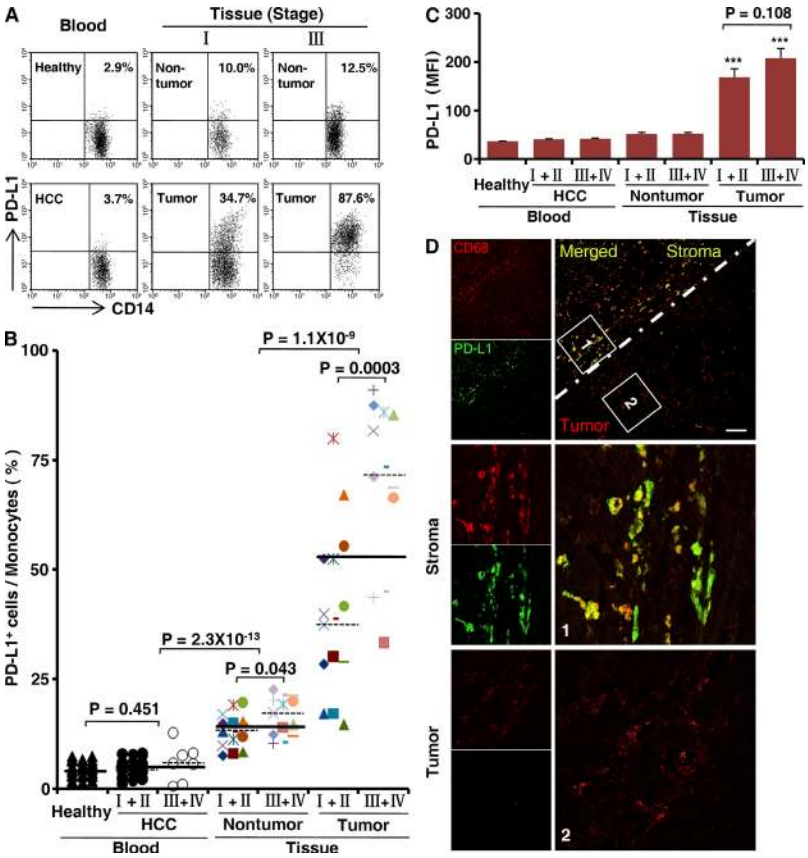


**Figure 1. Monocytes isolated from human HCC tumor tissue expressed PD-L1.** (A–C) FACS analysis of PD-L1 expression on fresh monocytes isolated from peripheral blood and tissues. The percentage of PD-L1$^{+}$CD14$^{high}$ monocytes (A and B) and the mean fluorescence intensity (MFI) of PD-L1$^{+}$CD14$^{high}$ cells (C) are shown. The numbers of samples collected from patients and donors in A–C were as follows: blood from 28 healthy individuals, and 21 stage I and II and 7 stage III and IV HCC patients; and paired nontumor and tumor tissue from 15 stage I and II and 13 stage III and IV HCC patients. The data shown in A are representative dot plots of at least seven individuals from more than five independent experiments; B and C show the statistical analysis of these samples. The continuous and dashed horizontal bars in B represent median values. Results are expressed as means ± SEM. (D) Analysis of PD-L1 distribution in HCC samples by confocal microscopy. The micrographs at higher magnification show the stained peritumoral stroma region (1) and a cancer nest (2). Significant difference compared with healthy blood is indicated (***, $P < 0.0001$). 1 out of 10 representative micrographs is shown in D. Bar, 50 µm.

### PD-L1 expression and activation of monocytes/Mφ are correlated in peritumoral stroma in HCC patients

The results described above suggested that monocytes are activated by tumor environments to express PD-L1 protein during the early migration/differentiation stage. To test this, we examined the coexpression of PD-L1 and HLA-DR on monocytes freshly isolated from peripheral blood, tumor, or nontumor liver tissues from HCC patients ($n$ = 28 for each group). Consistent with the results for PD-L1 expression, we observed a significantly increased percentage of $CD14^{high}$ cells with high HLA-DR intensity in the tumor tissues (63.3 ± 3.7%; $P < 0.001$ for all; Fig. 3, A–C), and a higher ratio of $HLA\text{-}DR^{high}CD14^{high}$ cells in monocytes was found in tumor masses from advanced stage HCC patients (stages III and IV [$n$ = 13] vs. stages I and II [$n$ = 15]; $P < 0.01$; Fig. 3 B). Approximately 90% of $HLA\text{-}DR^{high}CD14^{high}$ cells from tumors also expressed substantial amounts of PD-L1 ($n$ = 28). Moreover, significant correlations were found between the levels of $PD\text{-}L1^+$ and $HLA\text{-}DR^{high}$ monocytes in all of the samples analyzed ($n$ = 112; linear regression, r = 0.934; $P < 0.0001$; Fig. 3 D). The coexistence of HLA-DR and PD-L1 on monocytes/Mφ was further confirmed by examining expression of these proteins in serial sections of HCC tumor samples. As shown in Fig. 3 E, most of the $HLA\text{-}DR^{high}CD68$ cells were accumulated in the peritumoral stroma area, and they were also positive for PD-L1 ($n$ = 15). Of note, most infiltrating $CD8^+$ T cells were also located in the same area.

### High infiltration of peritumoral $PD\text{-}L1^+$ monocytes/Mφ is correlated with disease stage and poor survival of patients

Based on our observation that in tissues from advanced stage HCC patients high levels of PD-L1 protein were expressed by $CD68^+$ cells in peritumoral stroma, but not by those in intratumoral or nontumoral areas, we predicted that the presence of peritumoral $CD68^+$ cells would have an adverse effect on survival. To test this assumption, 262 HCC patients received curative resection with follow-up data and were divided into two groups according to the median value of peritumoral stroma CD68 density (low, ≤118 cells [$n$ = 134]; high, >119 cells [$n$ = 128]). There was a positive association between the densities of $CD68^+$ and $PD\text{-}L1^+$ cells in peritumoral stroma ($n$ = 35; linear regression, r = 0.783; $P < 0.01$; Fig. 4 A), but striking negative associations between the $CD68^+$ cell density in that area and overall survival (OS) and disease-free survival (DFS), respectively ($n$ = 262; $P < 0.01$ for both OS and DFS; Fig. 4 B). In contrast, $CD68^+$ cells in the nontumor area had no impact on the prognosis of either OS or DFS (unpublished data). Peritumoral stroma $CD68^+$ cell density was also associated with tumor size ($P = 0.032$), tumor multiplicity ($P = 0.003$), and tumor node metastasis stage ($P = 0.002$; Table S2). Multivariate analysis revealed that the number of

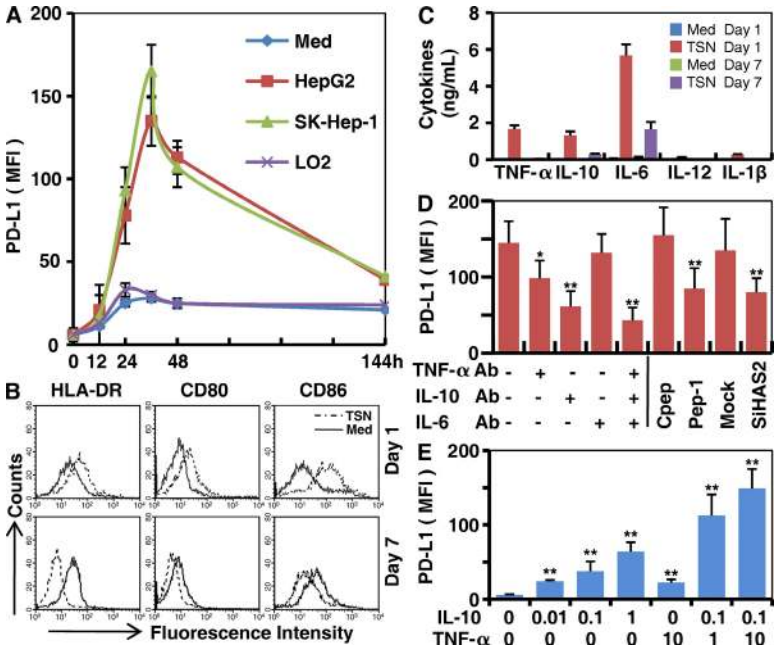


**Figure 2. Tumor environments regulated PD-L1 expression on monocytes/Mφ.** (A) Monocytes were left untreated or cultured with the indicated supernatants for different times. (B and C) Monocytes were left untreated or cultured with supernatant from SK-Hep-1 cells (TSN) for the indicated times. (D) Monocytes were left untreated or pretreated for 1 h with the indicated blocking antibodies, Pep-1, or control peptide (Cpep), and were then incubated for 24 h with SK-Hep-1 TSN. In parallel, some untreated monocytes were incubated for 24 h with TSNs from mock or SiHAS2 cells. (E) Monocytes were incubated for 24 h with rhIL-10 or rhTNF-α at the indicated concentrations (ng/ml). The MFI of PD-L1 and expression of surface markers were determined by FACS, and the production of cytokines was assessed by ELISA. The histograms in B are representative of five separate experiments. Values given in A, C, D, and E represent the means ± SE of four separate experiments. *, $P < 0.05$; and **, $P < 0.01$ indicate a significant difference from untreated TSN-exposed monocytes (D) or untreated monocytes (E).

$CD68^+$ cells in peritumoral stroma was an independent prognostic factor of OS (Table I). These results suggest that an increase in numbers of peritumoral stroma $CD68^+$ cells is correlated with progression of HCC and, therefore, might serve as an independent predictor of poor survival.

### Monocyte-associated PD-L1 suppresses tumor-specific T cell immunity

The colocalization of $PD\text{-}L1^+CD68^+$ cells and $CD8^+$ T cells in the peritumoral stroma of HCC tissues (Fig. 3 E) suggests that these monocytes/Mφ promote tumor progression by impairing T cell immunity. Therefore, our next objective was to determine the role of $PD\text{-}L1^+$ tumor monocytes in T cell suppression. Fig. 5 A shows that most of the $CD8^+$ T cells (78 ± 15%; $n = 15$) in peritumoral stroma were in close contact with $PD\text{-}L1^+$ cells. Interestingly, a significantly larger portion of the tumor-infiltrating cytotoxic cells expressed the PD-L1 receptor PD-1 (61 ± 11%; $n = 7$; $P < 0.001$ compared with nontumor-infiltrating T cells; Fig. 5, B and C), which suggests that tumor monocytes may regulate T cell function via PD-L1 signals. To address that possibility, we purified tumor monocytes (>50% of them were $PD\text{-}L1^+$) and autologous tumor-infiltrating T cells from HCC tissues, and then performed ELISPOT assays. The result showed that tumor T cells co-cultured with tumor monocytes exhibited an impaired production of IFN-γ. Consistent with our hypothesis, blockade of PD-L1 by preincubation of tumor monocytes with the mAb MIH1 (19, 20) could markedly enhance the ability of tumor T cells to produce IFN-γ (Fig. 5 D).

To further elucidate the effect of $PD\text{-}L1^+$ monocytes on T cell immunity, we generated one control T cell line stimulated

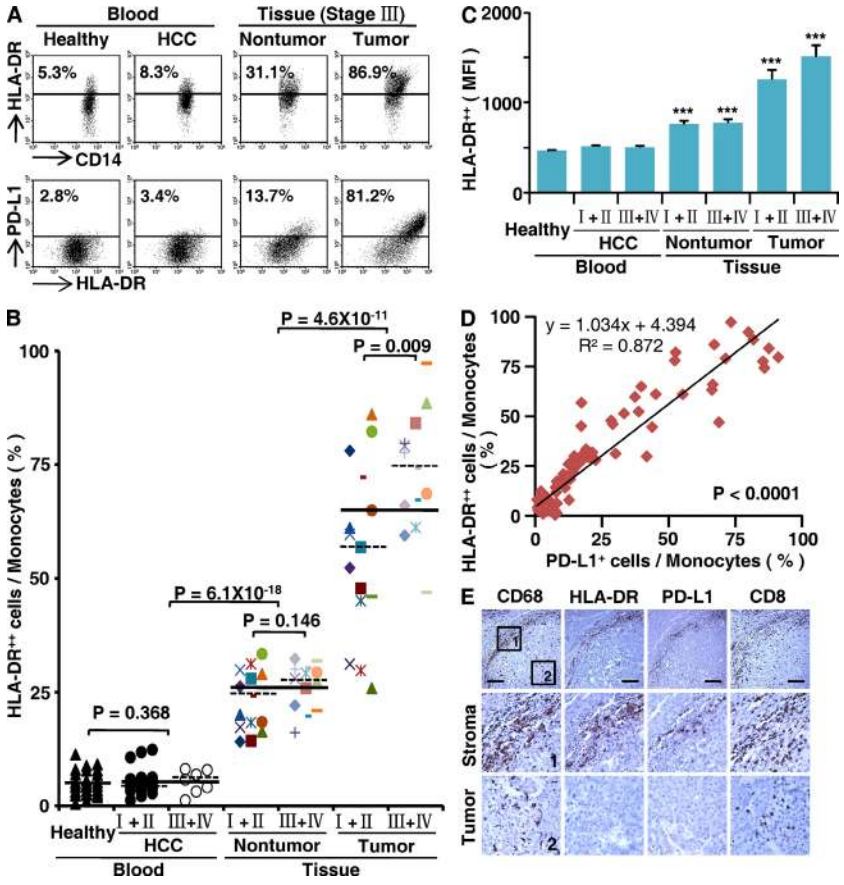


**Figure 3. Expression pattern of PD-L1 was correlated with the activation pattern of monocytes/Mφ in peritumoral stroma.** (A–C) FACS analysis of PD-L1 and HLA-DR expression in fresh monocytes isolated from peripheral blood and tissues. Representative data on $PD\text{-}L1^+HLA\text{-}DR^{high}$ monocytes (A), percentages of $HLA\text{-}DR^{high}CD14^{high}$ monocytes (B), and the MFI of HLA-DR in $HLA\text{-}DR^{high}CD14^{high}$ monocytes (C) are shown. The samples collected and the numbers of donors in A–C were the same as in Fig. 1. The data shown in A are representative dot plots of at least seven individuals from more than five independent experiments; B and C show the statistics analysis of these samples. The continuous and dashed horizontal bars in B represent median values. Results are expressed as means ± SEM. (D) Positive correlations between the levels of $PD\text{-}L1^+$ and $HLA\text{-}DR^{high}$ monocytes. The samples used in D were blood from healthy individuals, HCC patients, and paired nontumor and tumor tissues from HCC patients ($n = 28$ for each). (E) Adjacent sections of paraffin-embedded hepatoma samples stained with the indicated markers. The micrographs at higher magnification show the peritumoral stroma region (1) and a cancer nest (2). Significant difference compared with healthy blood is indicated (***, $P < 0.0001$). 1 out of 15 representative micrographs is shown in E. Bars, 150 µm.

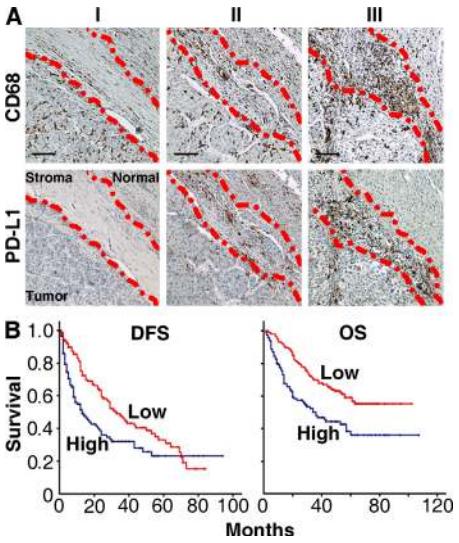


**Figure 4. Accumulation of PD-L1$^+$CD68$^+$ cells in peritumoral stroma predicted poor survival in HCC patients.** (A) Adjacent sections of paraffin-embedded hepatoma samples stained with an anti-CD68 or an anti–PD-L1 antibody. Different levels of Mφ infiltration can be seen along the peritumoral region: I, none or slight; II, moderate; and III, strong. The dashed lines represent the edges of tumor, stroma, or normal tissues. Bars, 50 µm. (B) OS and DFS in 262 HCC patients in relation to CD68 density in peritumoral stroma. The patients were divided into two groups according to the median value of CD68$^+$ Mφ density in peritumoral stroma: red lines, low density ($n$ = 134); blue lines, high density ($n$ = 128). Cumulative OS and DFS time were calculated by the Kaplan-Meier method and analyzed by the log-rank test.

with anti-CD3/CD28, and two types of tumor-reactive T cell lines with HepG2- and U937-loaded APCs, respectively (Fig. S1, A and B). Both tumor-reactive T cell lines can specifically inhibit the proliferation and exert their cytotoxicity against corresponding tumor cells, whereas the control T cell line hardly had any effect (Fig. S1, A and B). However, exposure to TSN-treated PD-L1$^+$ monocytes for 24 h induced dysfunctional T cells that had a low cytotoxicity as well as impaired capacities for proliferation, expression of the activation marker CD25, and production of IL-2 and IFN-γ (Fig. 6 and Fig. S1 C). Consistent with our hypothesis, blockade of PD-L1 significantly attenuated such T cell suppression mediated by TSN-treated monocytes (Fig. 6 and Fig. S1 C). Collectively, these findings show that PD-L1 contributes to tumor monocyte–mediated suppression in vitro.

### Blockade of monocyte-associated PD-L1 improves tumor-specific T cell immunity

To test the effect of monocyte PD-L1 on tumor-specific T cell immunity in vivo, we treated TSN-exposed PD-L1$^+$ monocytes with PD-L1 blocking or control antibody and then injected them together with autologous tumor-specific T cells into our established human nonobese diabetic/severe combined immunodeficiency (NOD/SCID) mice bearing HepG2-derived hepatoma. As expected, mice without T cell transfusions, mice treated with tumor-specific T cells plus PD-L1$^+$ monocytes or control antibody–treated PD-L1$^+$ monocytes, showed progressive tumor growth. Supporting our hypothesis that tumor monocyte PD-L1 signals are immunopathological in vivo, mice treated with tumor-specific T cells plus PD-L1 blocking antibody–treated monocytes showed reduced tumor volumes at each measurement time point from day 8 ($n$ = 4 mice per group; *, $P < 0.05$ compared with control antibody; Fig. 7). These data indicate that tumor monocytes defeat tumor-specific T cell immunity in vivo via PD-L1 signals and thereby contribute to tumor growth.

**Table I.** Univariate and multivariate analyses of factors associated with survival and recurrence

| | OS | | | | DFS | | | |
|---|---|---|---|---|---|---|---|---|
| | Univariate | Multivariate | | | Univariate | Multivariate | | |
| Variables | p-value | HR | 95% CI | p-value | p-value | HR | 95% CI | p-value |
| Age, years (>48 vs. ≤48) | 0.344 | | | NA | 0.643 | | | NA |
| Gender (female vs. male) | 0.461 | | | NA | 0.215 | | | NA |
| HbsAg (positive vs. negative) | 0.086 | | | NA | 0.127 | | | NA |
| Cirrhosis (present vs. absent) | 0.211 | | | NA | 0.09 | | | NA |
| ALT, U/L (>42 vs. ≤42) | 0.38 | | | NA | 0.883 | | | NA |
| AFP, ng/ml (>25 vs. ≤25) | 0.005 | 1.68 | 1.07–2.62 | 0.023 | 0.221 | | | NA |
| Tumor size, cm (>5 vs. ≤5) | 0.004 | 1.66 | 1.1–2.51 | 0.016 | 0.024 | 1.44 | 1–2.07 | 0.052 |
| Tumor multiplicity (multiple vs. solitary) | <0.001 | 1.32 | 0.61–2.84 | 0.485 | 0.017 | 1.11 | 0.55–2.23 | 0.773 |
| Vascular invasion (present vs. absent) | 0.002 | 2.1 | 1.19–3.74 | 0.011 | 0.006 | 1.88 | 1.1–3.23 | 0.022 |
| Intrahepatic metastasis (yes vs. no) | <0.001 | 2.18 | 1.06–4.5 | 0.035 | 0.007 | 1.58 | 0.79–3.16 | 0.195 |
| TNM stage (III+IV vs. I+II) | 0.014 | 0.68 | 0.37–1.26 | 0.219 | 0.034 | 0.96 | 0.56–1.63 | 0.869 |
| Tumor differentiation (III+IV vs. I+II) | 0.1 | | | NA | 0.308 | | | NA |
| Fibrous capsule (present vs. absent) | 0.263 | | | NA | 0.742 | | | NA |
| Peritumoral stroma Mφ (high vs. low) | <0.001 | 1.67 | 1.15–2.42 | 0.007 | 0.003 | 1.33 | 0.94–1.88 | 0.113 |

Cox proportional hazards regression model. Variables used in multivariate analysis were adopted by univariate analysis. The underlined terms represent statistical significance. AFP, α-fetoprotein; ALT, alanine aminotransferase; CI, confidence interval; HbsAg, hepatitis B surface antigen; HR, hazard ratio; NA, not adopted; TNM, tumor node metastasis.

## DISCUSSION

Much research has been focused on tumor-mediated immunosuppression over the past decade (4, 21). However, in spite of the generalized immunosuppressive status in cancer patients, many malignancies arise at sites of chronic inflammation, and inflammatory mediators are often produced in tumors (22–24). The present study demonstrates that the activated monocytes in a tumor microenvironment express PD-L1 (B7-H1) molecules to suppress tumor-specific T cell function, which may represent a novel link between proinflammatory response and immune tolerance in the tumor milieu.

Human tumor tissues can be anatomically classified into areas of intratumoral and peritumoral stroma, each with distinct compositions and functional properties (5, 7, 24, 25). Intratumoral environments usually contain abundant immunosuppressive molecules and cells to inhibit the T cell responses and create conditions that are conducive to tumor growth (21, 26–28). In contrast, the stromal areas in most tumors contain a significant amount of leukocyte infiltrate, which was long assumed to represent the host response to the malignancy. In the current study, we observed that monocytes in the peritumoral stroma had an activated phenotype with increased expression of HLA-DR, CD80, and CD86 (Fig. 3 and not depicted). Data from an in vitro study showed that such tumor-activated monocytes produced significant levels of proinflammatory cytokines, including IL-1β, IL-12, and TNF-α. However, these activated APCs were unable to stimulate effective antitumor T cell responses, and instead they suppressed the T cell immunity both in vitro and in vivo, which suggests that such monocytes can actually benefit tumor progression. This notion is supported by our finding that the density of monocytes/Mφ in peritumoral stroma was correlated with advanced disease stages and poor survival in HCC patients. Consistent with our results, other investigators have recently reported that the increased $CD68^+HLA\text{-}DR^+$ cells in peritumoral liver tissues are positively associated with metastatic potential in HCC (5).

Mφ are versatile, plastic cells that can respond to environmental signals through diverse functional programs (6, 29). We have recently shown that tumors dynamically regulate recruiting monocytes at distinct sites, which leads to transient activation of monocytes in peritumoral stroma and subsequent formation of suppressive Mφ in cancer nests (7). The present study provided evidence that a fraction of these activated monocytes express PD-L1, and that those cells significantly inhibit tumor-specific T cell proliferation, cytokine production, and cytotoxic potential in vitro. We also found that $PD\text{-}L1^+$ monocytes inhibited tumor-specific immunity in vivo and fostered tumor growth in NOD/SCID mice bearing human tumors. Several of our observations support

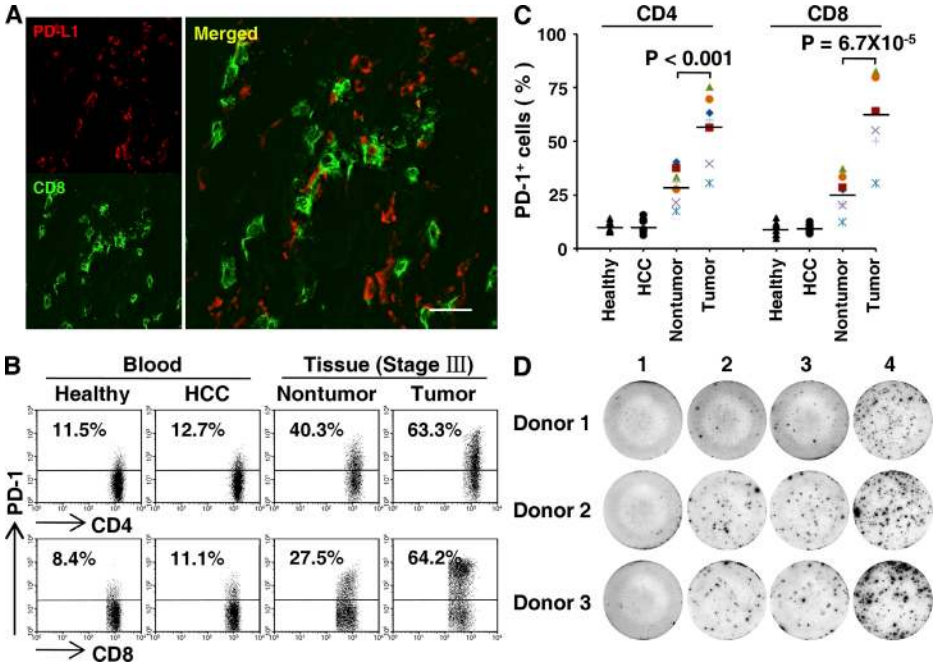


**Figure 5. Tumor-derived monocytes induced T cell suppression via PD-L1.** (A) Physical contact between $PD\text{-}L1^+$ cells (red) and $CD8^+$ cytotoxic T cells (green) in HCC peritumoral stroma. One out of five representative micrographs is shown in A. Bar, 20 µm. (B and C) Increased expression of PD-1 protein on the surface of tumor-infiltrating T cells from HCC patients. The samples used in B and C were fresh blood from healthy individuals and HCC patients, and paired nontumor and tumor tissues from HCC patients ($n = 7$ for each). The data shown in B are representative dot plots of seven patients from six independent experiments. The horizontal bars in C represent median values. (D) HCC-derived monocytes induced anergy of tumor T cells with reduced IFN-γ production. Purified tumor T cells were left untreated (1), or were incubated for 20 h with autologous tumor monocytes supplemented with 25 µg/ml of autologous tumor mass lysate in the absence (2) or presence of 5 µg/ml of control (3) or anti–PD-L1 antibody (4). Thereafter, production of IFN-γ was determined by ELISPOT. Three out of six representative patient samples are shown in D.

the notion that tumor monocyte PD-L1 signals contribute to immunopathology. First, tumor-activated monocytes in our experiments strongly expressed PD-L1 molecules with kinetics similar to their activation status, and significant correlations were found between the levels of PD-L1$^+$ and HLA-DR$^{high}$ on tumor-infiltrating monocytes. Second, these PD-L1–expressing monocytes effectively suppressed the tumor-specific T cell immunity, and that effect was attenuated by blocking PD-L1 on these monocytes. Third, expression of the PD-L1 receptor PD-1 was significantly increased on tumor-infiltrating T cells, and many of those cells were in close contact with activated PD-L1$^+$ monocytes in peritumoral stroma. Fourth, expression of PD-L1 on tumor-infiltrating monocytes was increased with HCC progression, and greater intensity of such protein was associated with high mortality and reduced survival in the patients. Therefore, expression of PD-L1 on activated monocytes may represent a novel mechanism that represses antitumor T cell immunity.

PD-L1 is a cell-surface glycoprotein belonging to the B7 family of cosignaling molecules with a profound regulatory effect on T cell responses (30–32). Studies in mouse models have revealed that expression of PD-L1 helped dormant tumor cells to evade cytotoxic T cell responses (33, 34). Although expression of PD-L1 protein is often found on activated cells and various human carcinomas, the regulatory mechanisms of human PD-L1 remain to be defined. We found that autocrine TNF-α and IL-10, but not IFN-γ, released

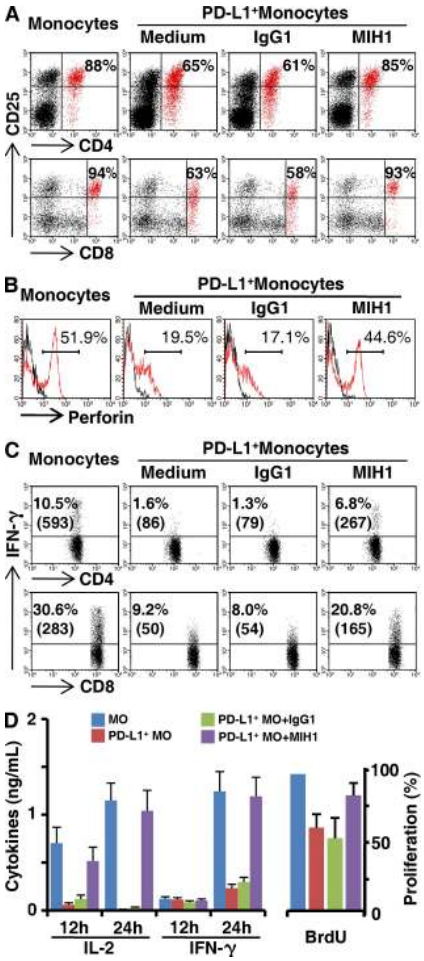


**Figure 6. TSN-exposed monocytes induced T cell suppression via PD-L1.** Autologous monocytes (MO) or TSN-treated monocytes (PD-L1$^+$ MO) were pretreated with 10 µg/ml mitomycin C for 30 min and were then washed and incubated with tumor-specific T cells (1:10) in the presence or absence of 5 µg/ml anti–PD-L1 or control antibody, as described in Materials and methods. The expression of CD25 on (A) T cells, (B) perforin in CD8$^+$ T cells, and (C) intracellular staining of IFN-γ were determined by FACS, and (D) the secretion of cytokines and proliferation of T cells were determined by ELISA and BrdU assay, respectively. The results shown are representative of at least four separate experiments and are expressed as means ± SEM. Significant differences compared with normal monocytes are indicated (*, $P < 0.05$; and **, $P < 0.01$).

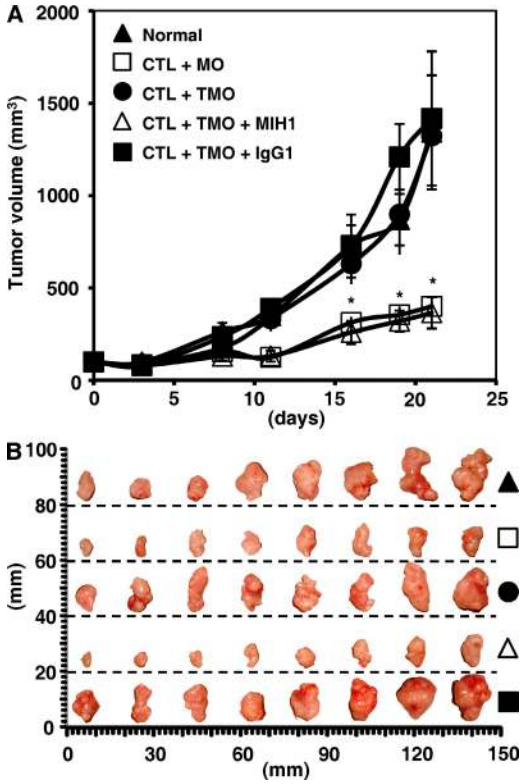


**Figure 7. Blockade of PD-L1 improved monocyte-mediated T cell activation in vivo.** (A) Blocking PD-L1 in TSN-conditioned monocytes results in tumor regression in vivo. Mice were injected with human HepG2 cells, as described in Materials and methods. The control animals (▲) received no further injections. The experimental treatments entailed injections with tumor-specific T cells in combination with untreated monocytes (□) or TSN-exposed monocytes (●), or TSN-exposed monocytes pretreated with an anti–PD-L1 antibody (△) or a control antibody (■). The illustrated data represent means ± SD of tumor volumes ($n = 8$ tumors in each group of four mice). The day of T cell injection was counted as day 0. The results shown in A are representative of three separate experiments and are expressed as means ± SEM. *, $P < 0.05$ compared with control antibody. CTL, tumor-specific T cells; MO, monocytes; TMO, TSN-exposed monocytes. (B) The tumors were excised and photographed 21 d after injecting the cells. One out of three separate experiments is shown in B.

from activated monocytes, stimulated monocyte PD-L1 expression. Furthermore, in vitro study using recombinant TNF-α and IL-10 indicated that IL-10 was essential for PD-L1 induction and that proinflammatory TNF-α acted synergistically with antiinflammatory IL-10 to enhance PD-L1 expression on monocytes. Moreover, comparison of the kinetics of cytokine production (7) and PD-L1 expression (Fig. 2 A) in TSN-treated monocytes revealed that accumulation of TNF-α and IL-10 preceded the up-regulation of PD-L1. Such sequential cytokine production and PD-L1 expression on TSN-activated monocytes may reflect a novel immune-editing mechanism by which tumors render activated monocytes to perform a suppressive role by stimulating PD-L1 expression. This hypothesis is compatible with previous studies showing that the proinflammatory cytokines IL-1β or TNF-α can significantly enhance IFN-γ–dependent indoleamine 2,3-dioxygenase expression on epithelial cells (35, 36).

In addition to PD-L1, another member of the B7 family, B7-H4, is also selectively expressed by various cellular components in the tumor microenvironment (4, 28). High levels of B7-H4 have been detected on a fraction of tumor-associated Mφ in patients with ovarian carcinoma, and these B7-H4$^+$ Mφ were found to inhibit tumor-specific T cell effector function both in vitro and in vivo (37). Moreover, regulatory T cells can trigger production of IL-10 by APCs, which in turn stimulates such cells to express B7-H4 in an autocrine manner and renders them immunosuppressive via the B7-H4 molecules (38). Therefore, manipulating the expression of and signaling through these molecules may open new avenues for developing novel immune-based therapies to enhance antitumor immunity in human cancer (39, 40).

Emerging evidence indicates that it is not inflammation per se but inflammatory "context" that determines the ability of proinflammatory factors to facilitate or prevent tumor growth. Our results suggest that there is fine-tuned collaborative action between immune activation and immunosuppression in tumor microenvironments. Soluble factors derived from cancer cells can trigger transient activation of newly recruited monocytes in the peritumoral stroma area, and thereby induce the monocytes to produce significant amount of cytokines, including TNF-α and IL-10, which in turn leads to the expression of PD-L1 (B7-H1) protein on their surface and ultimately impairs the antitumor T cell immunity. These findings provide important new insight into the significance about how activated monocytes in tumors may perform a suppressive role by stimulating PD-L1 (B7-H1) expression, which would be helpful for the rational design of novel immune-based anticancer therapies.

## MATERIALS AND METHODS

**Patients and specimens.** Tumor or peripheral blood samples were obtained from 312 untreated patients with pathologically confirmed HCC at the Sun Yat-Sen University Cancer Center. Of these, 262 patients who underwent curative resection between 1999 and 2004 (designated Group 1) had complete follow-up data, and they were further enrolled for analysis of OS and DFS. Clinical stages were classified according to the International Union against Cancer. Blood samples from 28 patients as well as fresh tumor and nontumor (at least 3 cm away from the tumor site) tissues from 28 patients (Group 2) were used for the isolation of peripheral leukocytes, and tumor- and nontumor-infiltrating leukocytes. The clinical characteristics of all patients are summarized in Table S3.

Control blood samples were obtained from 28 healthy blood donors attending the Guangzhou Blood Center, all of whom were negative for antibodies against hepatitis C virus, hepatitis B virus, HIV, and syphilis. All samples were anonymously coded in accordance with local ethical guidelines (as stipulated by the Declaration of Helsinki), and written informed consent was obtained and the protocol was approved by the Review Board of Sun Yat-Sen University Cancer Center.

**Isolation of mononuclear cells from peripheral blood and tissues.** Peripheral leukocytes were isolated by Ficoll density gradient centrifugation (7). Fresh tumor- and nontumor-infiltrating leukocytes were obtained as previously described (41). In short, liver biopsy specimens ($n = 28$) were cut into small pieces and digested in RPMI 1640 supplemented with 0.05% collagenase IV (Sigma-Aldrich), 0.002% DNase I (Roche), and 20% FCS (HyClone Laboratories) at 37°C for 20 min. Dissociated cells were filtered through a 150-μm mesh and separated by Ficoll centrifugation. The mononuclear cells were washed and resuspended in medium supplemented with 1% heat-inactivated FCS for FACS analysis.

**ELISPOT assay.** Tumor monocytes and T cells were purified from HCC-infiltrating leukocytes in a MACS column purification system (Miltenyi Biotec). ELISPOT assays were performed using a commercial set (BD) according to the manufacturer's instructions. In brief, 96-well nitrocellulose plates (Millipore) were coated with 5 μg/ml anti–human IFN-γ capture antibody at 4°C overnight. The wells were then washed and blocked for 2 h at room temperature with 10% FBS–RPMI 1640 medium. $10^5$ purified tumor T cells were left untreated or cultured with autologous tumor monocytes (5:1) in the presence of 25 μg/ml of tumor mass lysates and incubated for 20 h. After wash, the plates were incubated with 2 μg/ml of biotinylated anti–human IFN-γ detection antibody and developed with streptavidin–horseradish peroxidase, followed by the addition of 3-amino-9-ethylcarbazole substrate reagent.

**Flow cytometry.** Peripheral blood leukocytes and tumor- and nontumor-infiltrating leukocytes were stained with fluorochrome-conjugated mAbs against PD-L1, CD14, CD80, CD86, or HLA-DR, or control antibodies (BD or eBioscience) according to the manufacturer's instructions, and they were subsequently analyzed by multicolor flow cytometry.

**Cell lines and preparation of TSNs.** Human hepatoma (SK-Hep-1 and HepG2) cell lines were obtained from American Type Culture Collection; normal liver (LO2) cells were obtained from the Institute of Biochemistry and Cell Biology at the Chinese Academy of Sciences; and the stable hyaluronan synthase 2–knockdown SK-Hep-1 clones (SiHAS2) and the mock transfectants were established in our previous study (7, 42). All cells were tested for mycoplasma contamination using a single-step PCR method (43), and they were maintained in DMEM supplemented with 10% FCS. TSNs were prepared as previously described (7, 16).

**Regulation of PD-L1 expression.** Fresh blood monocytes were cultured for the indicated times with TSNs or different concentrations of rhIL-10 and rhTNF-α (R & D Systems). In some experiments, before exposure to TSNs, the cells were pretreated with neutralizing mAbs against 20 μg/ml IL-6, 10 μg/ml IL-10, or 1 μg/ml TNF-α (R & D Systems), or with hyaluronan-blocking peptide (200 μg/ml pep-1; GL Biochem). Cells were subject to FACS analysis to detect surface PD-L1 protein, and the levels of TNF-α, IL-12p70, IL-1β, IL-6, and IL-10 in culture supernatants were detected by ELISA (eBioscience).

**Immunohistochemistry and immunofluorescence.** Paraffin-embedded and formalin-fixed samples were cut into 5-μm sections, which were then processed for immunohistochemistry as previously described (7). After

incubation with an antibody against human CD8 (Thermo Fisher Scientific), CD68 (Dako), HLA-DR (R&D Systems), or PD-L1 (MIH1; eBioscience), the adjacent sections were stained with diaminobenzidine or 3-amino-9-ethylcarbazole in an Envision System (Dako). For immunofluorescence analysis, tissues were stained with polyclonal rabbit anti–human CD8 and mouse anti–human PD-L1, or rabbit anti–human CD68 (Santa Cruz Biotechnology, Inc.) and mouse anti–human PD-L1, followed by Alexa Fluor 488– or 568–conjugated goat anti–mouse IgG and Alexa Fluor 568– or 488–conjugated goat anti–rabbit IgG (Invitrogen). Positive cells were quantified using ImagePro Plus software (Media Cybernetics) and expressed as the mean of the percentage of positive cells ± SD in 10 high-powered fields detected by confocal microscopy (16, 37).

**Evaluation of immunohistochemical variables.** Analysis was performed by two independent observers who were blinded to the clinical outcome. At low power (×100), the tissue sections were screened using an inverted research microscope (model DM IRB; Leica), and the five most representative fields were selected. Thereafter, to evaluate the density of $CD68^+$ Mφ, the respective areas of peritumoral stroma were measured at ×400 magnification, and the nucleated $CD68^+$ Mφ in each area were counted and expressed as the number of cells per field.

**In vitro tumor-specific T cell immunosuppression.** Monocyte-derived DCs were incubated with irradiated apoptotic HepG2 or U937 cells at a 1:5 ratio for 24 h. Autologous blood CD3 T cells ($2 \times 10^5$ cells/well in 96-well plates; Pan T cell kit; Miltenyi Biotec) were activated by incubation with those tumor-loaded DCs ($2 \times 10^4$ cells/well) in the presence of 10 U/ml IL-2 (11, 37) and 10 ng/ml IL-7 for 2 wk. Thereafter, a second stimulation was performed by further incubation with tumor-loaded DCs for another 2 wk to generate tumor-specific T cells. The control T cell lines were generated via polyclonal stimulations (2.5 μg/ml anti-CD3 and -CD28). The specificity of T cells was examined in Fig. S1 (A and B). Autologous or TSN-treated monocytes were pretreated with 10 μg/ml mitomycin C (Sigma-Aldrich) for 30 min, washed twice, and co-cultured for 24 h with polyclonal-stimulated (0.5 μg/ml anti-CD3 and 0.1 μg/ml anti-CD28) tumor-specific T cells at a ratio of 1:10 in the presence or absence of 5 μg/ml anti–human PD-L1 antibody, and BrdU (Roche) was present during the final 5 h. The production of cytokines and proliferation of cells were detected by ELISA. In some experiments, 10 μg/ml brefeldin A (Sigma-Aldrich) was added to the culture for the final 5 h, and the intracellular cytokines were determined by FACS.

**In vivo tumor regression assay.** Animal protocols were approved by the Review Board of Sun Yat-Sen University Cancer Center. $10^6$ hepatoma cells (HepG2) in 100 μl of buffered saline were subcutaneously injected into the dorsal tissues of male NOD/SCID mice (5–7 wk old, two tumors per mouse). $5 \times 10^6$ tumor-specific T cells were conditioned with monocytes or TSN-treated monocytes in the presence or absence of PD-L1 antibody, as described in the previous section, and were subsequently injected into the peritoneum in 100 μl of buffered saline on day 7 after inoculation. Tumor size was measured twice weekly by two independent observers using calipers fitted with a vernier scale. Tumor volume was calculated based on three perpendicular measurements (37).

**Statistical analysis.** Results are expressed as means ± SEM. The statistical significance of differences between groups was determined by the Student's *t* test. Correlations between parameters were assessed using the Pearson correlation analysis and linear regression analysis, as appropriate. Cumulative survival time was calculated by the Kaplan-Meier method, and survival was measured in months from resection to recurrence or the last review. The log-rank test was applied to compare the groups. Multivariate analysis of prognostic factors for OS and DFS were performed using the Cox proportional hazards model. SPSS statistical software (version 13.0) was used for all statistical analyses. All data were analyzed using two-tailed tests unless otherwise specified, and $P < 0.05$ was considered statistically significant.

**Online supplemental material.** Fig. S1 shows the regulation of T cell cytotoxicity by TSN-exposed $PD\text{-}L1^+$ monocytes. Table S1 summarizes the blocking effects of IL-10, TNF-α, and IL-6 in the co-culture system by use of specific mAbs. Table S2 shows the association of peritumoral stroma CD68 cells with clinicopathological characteristics. Table S3 lists the clinical characteristics of 312 patients with HCC. Online supplemental material is available at http://www.jem.org/cgi/content/full/jem.20082173/DC1.

We thank P. Ödman for linguistic revision of the manuscript and G. Zhang for help with confocal microscopy.

This work was supported by the Outstanding Young Scientist Fund and project grants from the National Natural Science Foundation of China (30425025, 30672388, and 30730086), the "973" Program (2004CB518801), and the Ministry of Health of China (2008ZX10002-019).

The authors declare no competing financial interests.

**Submitted: 29 September 2008**
**Accepted: 27 April 2009**

## REFERENCES

1. Mueller, M.M., and N.E. Fusenig. 2004. Friends or foes - bipolar effects of the tumor stroma in cancer. *Nat. Rev. Cancer.* 4:839–849.
2. Tlsty, T.D., and L.M. Coussens. 2006. Tumor stroma and regulation of cancer development. *Annu. Rev. Pathol.* 1:119–150.
3. Ahmed, F., J.C. Steele, J.M. Herbert, N.M. Steven, and R. Bicknell. 2008. Tumor stroma as a target in cancer. *Curr. Cancer Drug Targets.* 8:447–453.
4. Zou, W., and L. Chen. 2008. Inhibitory B7-family molecules in the tumor microenvironment. *Nat. Rev. Immunol.* 8:467–477.
5. Budhu, A., M. Forgues, Q.H. Ye, H.L. Jia, P. He, K.A. Zanetti, U.S. Kammula, Y. Chen, L.X. Qin, Z.Y. Tang, and X.W. Wang. 2006. Prediction of venous metastases, recurrence, and prognosis in hepatocellular carcinoma based on a unique immune response signature of the liver microenvironment. *Cancer Cell.* 10:99–111.
6. Gordon, S., and P.R. Taylor. 2005. Monocyte and macrophage heterogeneity. *Nat. Rev. Immunol.* 5:953–964.
7. Kuang, D.M., Y. Wu, N. Chen, J. Cheng, S.M. Zhuang, and L. Zheng. 2007. Tumor-derived hyaluronan induces formation of immunosuppressive macrophages through transient early activation of monocytes. *Blood.* 110:587–595.
8. Lewis, C.E., and J.W. Pollard. 2006. Distinct role of macrophages in different tumor microenvironments. *Cancer Res.* 66:605–612.
9. Subudhi, S.K., P. Zhou, L.M. Yerian, R.K. Chin, J.C. Lo, R.A. Anders, Y. Sun, L. Chen, Y. Wang, M.L. Alegre, and Y.X. Fu. 2004. Local expression of B7-H1 promotes organ-specific autoimmunity and transplant rejection. *J. Clin. Invest.* 113:694–700.
10. Zang, X., and J.P. Allison. 2007. The B7 family and cancer therapy: costimulation and coinhibition. *Clin. Cancer Res.* 13:5271–5279.
11. Curiel, T.J., S. Wei, H. Dong, X. Alvarez, P. Cheng, P. Mottram, R. Krzysiek, K.L. Knutson, B. Daniel, M.C. Zimmermann, et al. 2003. Blockade of B7-H1 improves myeloid dendritic cell-mediated antitumor immunity. *Nat. Med.* 9:562–567.
12. Dong, H., S.E. Strome, D.R. Salomao, H. Tamura, F. Hirano, D.B. Flies, P.C. Roche, J. Lu, G. Zhu, K. Tamada, et al. 2002. Tumor-associated B7-H1 promotes T-cell apoptosis: a potential mechanism of immune evasion. *Nat. Med.* 8:793–800.
13. Thompson, R.H., and E.D. Kwon. 2006. Significance of B7-H1 overexpression in kidney cancer. *Clin. Genitourin. Cancer.* 5:206–211.
14. Llovet, J.M., A. Burroughs, and J. Bruix. 2003. Hepatocellular carcinoma. *Lancet.* 362:1907–1917.
15. Freeman, G.J., A.J. Long, Y. Iwai, K. Bourque, T. Chernova, H. Nishimura, L.J. Fitz, N. Malenkovich, T. Okazaki, M.C. Byrne, et al. 2000. Engagement of the PD-1 immunoinhibitory receptor by a novel B7 family member leads to negative regulation of lymphocyte activation. *J. Exp. Med.* 192:1027–1034.
16. Kuang, D.M., Q. Zhao, J. Xu, J.P. Yun, C. Wu, and L. Zheng. 2008. Tumor-educated tolerogenic dendritic cells induce CD3epsilon down-regulation and apoptosis of T cells through oxygen-dependent pathways. *J. Immunol.* 181:3089–3098.

17. Jiang, D., J. Liang, J. Fan, S. Yu, S. Chen, Y. Luo, G.D. Prestwich, M.M. Mascarenhas, H.G. Garg, D.A. Quinn, et al. 2005. Regulation of lung injury and repair by Toll-like receptors and hyaluronan. *Nat. Med.* 11:1173–1179.
18. Mummert, M.E., M. Mohamadzadeh, D.I. Mummert, N. Mizumoto, and A. Takashima. 2000. Development of a peptide inhibitor of hyaluronan-mediated leukocyte trafficking. *J. Exp. Med.* 192:769–779.
19. Saudemont, A., N. Jouy, D. Hetuin, and B. Quesnel. 2005. NK cells that are activated by CXCL10 can kill dormant tumor cells that resist CTL-mediated lysis and can express B7-H1 that stimulates T cells. *Blood.* 105:2428–2435.
20. Liu, J., A. Hamrouni, D. Wolowiec, V. Coiteux, K. Kuliczkowski, D. Hetuin, A. Saudemont, and B. Quesnel. 2007. Plasma cells from multiple myeloma patients express B7-H1 (PD-L1) and increase expression after stimulation with IFN-{gamma} and TLR ligands via a MyD88-, TRAF6-, and MEK-dependent pathway. *Blood.* 110:296–304.
21. Rabinovich, G.A., D. Gabrilovich, and E.M. Sotomayor. 2007. Immunosuppressive strategies that are mediated by tumor cells. *Annu. Rev. Immunol.* 25:267–296.
22. Karin, M., T. Lawrence, and V. Nizet. 2006. Innate immunity gone awry: linking microbial infections to chronic inflammation and cancer. *Cell.* 124:823–835.
23. Coussens, L.M., and Z. Werb. 2002. Inflammation and cancer. *Nature.* 420:860–867.
24. Vakkila, J., and M.T. Lotze. 2004. Inflammation and necrosis promote tumour growth. *Nat. Rev. Immunol.* 4:641–648.
25. Finak, G., N. Bertos, F. Pepin, S. Sadekova, M. Souleimanova, H. Zhao, H. Chen, G. Omeroglu, S. Meterissian, A. Omeroglu, et al. 2008. Stromal gene expression predicts clinical outcome in breast cancer. *Nat. Med.* 14:518–527.
26. Reichert, T.E., C. Scheuer, R. Day, W. Wagner, and T.L. Whiteside. 2001. The number of intratumoral dendritic cells and zeta-chain expression in T cells as prognostic and survival biomarkers in patients with oral carcinoma. *Cancer.* 91:2136–2147.
27. Fu, J., D. Xu, Z. Liu, M. Shi, P. Zhao, B. Fu, Z. Zhang, H. Yang, H. Zhang, C. Zhou, et al. 2007. Increased regulatory T cells correlate with CD8 T-cell impairment and poor survival in hepatocellular carcinoma patients. *Gastroenterology.* 132:2328–2339.
28. Zou, W. 2005. Immunosuppressive networks in the tumour environment and their therapeutic relevance. *Nat. Rev. Cancer.* 5:263–274.
29. Mantovani, A., S. Sozzani, M. Locati, P. Allavena, and A. Sica. 2002. Macrophage polarization: tumor-associated macrophages as a paradigm for polarized M2 mononuclear phagocytes. *Trends Immunol.* 23:549–555.
30. Keir, M.E., M.J. Butte, G.J. Freeman, and A.H. Sharpe. 2008. PD-1 and its ligands in tolerance and immunity. *Annu. Rev. Immunol.* 26:677–704.
31. Greenwald, R.J., G.J. Freeman, and A.H. Sharpe. 2005. The B7 family revisited. *Annu. Rev. Immunol.* 23:515–548.
32. Dong, H., G. Zhu, K. Tamada, and L. Chen. 1999. B7-H1, a third member of the B7 family, co-stimulates T-cell proliferation and interleukin-10 secretion. *Nat. Med.* 5:1365–1369.
33. Lukens, J.R., M.W. Cruise, M.G. Lassen, and Y.S. Hahn. 2008. Blockade of PD-1/B7-H1 interaction restores effector CD8+ T cell responses in a hepatitis C virus core murine model. *J. Immunol.* 180:4875–4884.
34. Pentcheva-Hoang, T., L. Chen, D.M. Pardoll, and J.P. Allison. 2007. Programmed death-1 concentration at the immunological synapse is determined by ligand affinity and availability. *Proc. Natl. Acad. Sci. USA.* 104:17765–17770.
35. Mellor, A.L., and D.H. Munn. 2004. IDO expression by dendritic cells: tolerance and tryptophan catabolism. *Nat. Rev. Immunol.* 4:762–774.
36. Babcock, T.A., and J.M. Carlin. 2000. Transcriptional activation of indoleamine dioxygenase by interleukin 1 and tumor necrosis factor alpha in interferon-treated epithelial cells. *Cytokine.* 12:588–594.
37. Kryczek, I., L. Zou, P. Rodriguez, G. Zhu, S. Wei, P. Mottram, M. Brumlik, P. Cheng, T. Curiel, L. Myers, et al. 2006. B7-H4 expression identifies a novel suppressive macrophage population in human ovarian carcinoma. *J. Exp. Med.* 203:871–881.
38. Kryczek, I., S. Wei, L. Zou, G. Zhu, P. Mottram, H. Xu, L. Chen, and W. Zou. 2006. Cutting edge: induction of B7-H4 on APCs through IL-10: novel suppressive mode for regulatory T cells. *J. Immunol.* 177:40–44.
39. Melero, I., I. Martinez-Forero, J. Dubrot, N. Suarez, A. Palazón, and L. Chen. 2009. Palettes of vaccines and immunostimulatory monoclonal antibodies for combination. *Clin. Cancer Res.* 15:1507–1509.
40. Guiducci, C., A.P. Vicari, S. Sangaletti, G. Trinchieri, and M.P. Colombo. 2005. Redirecting in vivo elicited tumor infiltrating macrophages and dendritic cells towards tumor rejection. *Cancer Res.* 65:3437–3446.
41. Unitt, E., S.M. Rushbrook, A. Marshall, S. Davies, P. Gibbs, L.S. Morris, N. Coleman, and G.J. Alexander. 2005. Compromised lymphocytes infiltrate hepatocellular carcinoma: the role of T-regulatory cells. *Hepatology.* 41:722–730.
42. Cheng, J., D.H. Huo, D.M. Kuang, J. Yang, L. Zheng, and S.M. Zhuang. 2007. Human macrophages promote the motility and invasiveness of osteopontin-knockdown tumor cells. *Cancer Res.* 67:5141–5147.
43. Uphoff, C.C., and H.G. Drexler. 2002. Detection of mycoplasma in leukemia-lymphoma cell lines using polymerase chain reaction. *Leukemia.* 16:289–293.